Employment of different turbulence models to the design of optimum steel flows in a tundish

Pradeep K. Jha and Sukanta K. Dash
Department of Mechanical Engineering, Indian Institute of Technology, Kharagpur, India

Received September 2002
Revised September 2003
Accepted September 2003

Keywords *Turbulence, Optimization techniques, Modelling*

Abstract *The Navier-Stokes equation and the species continuity equation have been solved numerically in a boundary fitted coordinate system comprising the geometry of a large scale industrial size tundish. The solution of the species continuity equation predicts the time evolution of the concentration of a tracer at the outlets of a six strand billet caster tundish. The numerical prediction of the tracer concentration has been made with six different turbulence models (the standard k-ε, the k-ε RNG, the Low Re number Lam-Bremhorst model, the Chen-Kim high Re number model (CK), the Chen-Kim low Re number model (CKL) and the simplest constant effective viscosity model (CEV)) which favorably compares with that of the experimental observation for a single strand bare tundish. It has been found that the overall comparison of the k-ε model, the RNG, the Lam-Bremhorst and the CK model is much better than the CKL model and the CEV model as far as gross quantities like the mean residence time and the ratio of mixed to dead volume are concerned. However, the k-ε model predicts the closest value to the experimental observation compared to all other models. The prediction of the transient behavior of the tracer is best done by the Lam-Bremhorst model and then by the RNG model, but these models do not predict the gross quantities that accurately like the k-ε model for a single strand bare tundish. With the help of the above six turbulence models mixing parameters such as the ratio of mix to dead volume and the mean residence time were computed for the six strand tundish for different outlet positions, height of advanced pouring box (APB) and shroud immersion depth. It was found that three turbulence models show a peak value in the ratio of mix to dead volume when the outlets were placed at 200 mm away from the wall. An APB was put on the bottom of the tundish surrounding the inlet jet when the outlets were kept at 200 mm away from the wall. It was also found that there exists an optimum height of the APB where the ratio of mix to dead volume and the mean residence time attain further peak values signifying better mixing in the tundish. At this optimum height of the APB, the shroud immersion depth was made to change from 0 to 400 mm. It was also observed that there exists an optimum immersion depth of the shroud where the ratio of mix to dead volume still attains another peak signifying still better mixing. However, all the turbulence models do not predict the same optimum height of the APB and the same shroud immersion depth as the optimum depth. The optimum height of the APB and the shroud immersion depth were decided when two or more turbulence models predict the same values.*

Nomenclature

C	= concentration of tracer	k	= turbulent kinetic energy
CV/Q	= dimensionless concentration	p	= pressure
C_{av}	= average concentration of the tracer at outlet i ($i = 1, 2, 3$)	Q	= volume of the tracer added
		t	= time

The second author, SKD, gratefully acknowledges the support of the Alexander von Humboldt Foundation for donating a high end PC on which the present computations were carried out, along with the preparation of the manuscript.

International Journal of Numerical Methods for Heat & Fluid Flow
Vol. 14 No. 8, 2004
pp. 953-979

0961-5539
DOI 10.1108/09615530410544283

t/τ = dimensionless time
t_r = actual mean residence time of fluid in the vessel, equation (7)
U = mean velocity
V = volume of the tundish
w' = fluctuating velocity of w component of mean velocity
x = coordinate for measure of distance
ρ = density of the fluid
μ = co-efficient of viscosity
ν = kinematic viscosity
$\overline{u_i u_j}$ = average turbulent stress
ε = rate of dissipation of turbulent kinetic energy
σ_c = turbulent Schmidt number
τ = theoretical mean residence time, Equation (6)
ϕ = either k or ε

Suffix

i, j, k = three Cartesian coordinate directions x, y and z
d = dead volume
m = mixed volume
p = plug volume

Introduction

The standard high Reynolds number k-ε turbulence model has been widely used in industrial applications to predict the overall performance of a device. The model has been proved to be very robust and economical from the view point of computer time because of the use of standard wall functions. However, it has been observed that in recirculating flow, the prediction of near wall quantity using the k-ε model does not compare very well with other low Reynolds number models. So for accurate prediction of overall quantity (mean residence time, mix volume and dead volume) in a device, modified forms of the standard k-ε model have been developed in the last decade. However, the use of such modified k-ε models has not been made very extensively for industrial cases excepting its validation with simple experiments. It has been the main motivation of the present work to use the standard k-ε model of Launder and Spalding (1972) along with its four modifications, RNG (Yahkot and Orszag, 1992), the Lam and Bremhorst (1981), Chen-Kim high Re number (CK) (Monson *et al.*, 1990) and Chen-Kim low Re number model (CKL)[1] to predict the mixing in a single and multi strand (multi exit) tundish which is a reasonably complex shaped device (when fitted with baffles, advanced pouring box and shroud) and plays a very important role in the steel industries for casting quality steel. The tundish is the last device in the sequential operation of steelmaking where final controls can be made to improve the quality of steel and decide on its final chemistry. Hence, fluid flow and mixing in a tundish have been studied by many authors, both numerically and experimentally (Debroy and Sychterz, 1985; He and Sahai, 1987; Madias *et al.*, 1999; Szekely *et al.*, 1987; Tacke and Ludwig, 1987; Xintian *et al.*, 1992; Yeh *et al.*, 1992). However, all the mathematical models of the past have used the standard k-ε model to solve the velocity field in the tundish and predict tracer concentration henceforth. The effects of various turbulence models on mixing have not been reported or compared with the experimental measurements taken in a tundish. Moreover, the effect of outlet positions, effect of height of advanced pouring box (APB) and the shroud immersion depth on mixing for a multi-strand tundish have not been reported by using various turbulence models. Jha and Dash (2002) and Jha *et al.* (2001) have reported the effect of outlet positions on mixing by using the standard k-ε model, the RNG and the Lam-Bremhorst model and the present work is an extension of their work where various turbulence models

are tried to examine the effect of the height of APB and the shroud immersion depth on mixing in a tundish.

Physical description of the problem

The geometry of the multi strand tundish is shown in Figure 1(a) along with three outlets. Half of the tundish is shown because of the symmetry about the inlet plane. The depth of the tundish and the bottom pad are 572 and 280 mm, respectively, with the size of the inlet as 25 mm × 50 mm and all other dimensions are shown in a plan view in Figure 2, which completes the detail geometrical description of the industrial size tundish taken for the mathematical simulation. It is to be noted that the outlets (15 mm × 15 mm) are drilled through the bottom pad at the positions shown and they have a length of 280 mm similar to the thickness of the bottom pad. The positions of the outlets are measured from the bottom wall and the exact locations of the outlets are shown in Figure 2. At position-1 the outlets are placed 50 mm away from the wall while at position-3 the outlets are 300 mm away from the wall. Mixing in the tundish is studied by injecting a dye through the inlet stream for a very short time and then computing the mass concentration of the dye in the entire tundish as a function of time. The intention is to compute the ratio of mix to dead volume and the mean residence time in the tundish by using various turbulence models, which are regarded as the main parameters for deciding the effective utilization of the tundish volume and hence mixing in the tundish. Also the response of the dye at all the outlets is monitored which in turn helps to compute the mixed and dead volume as well as the mean residence time (Jha *et al.*, 2001; Levenspiel, 1972; Szekely and Themelis, 1971). The objective is to find out a suitable location of the outlets, which can induce the highest possible mixing in a tundish and to study the effect of the outlet positions by using different turbulence models. An APB is normally put on the bottom of the tundish so that the inlet jet after striking the bottom pad cannot move straight towards the outlet thus avoiding proper mixing in a tundish (Figure 1(c)). The APB will cause the inlet stream to rise up after striking the bottom thus, inducing better mixing in a tundish. The inlet jet comes from the shroud tip and can pierce into the free surface of the tundish, but by this way the liquid picks up lot of atmospheric oxygen, which is not a desirable phenomenon for steel production. So the shroud extends into the free surface of the liquid steel (Figure 1(d)) and the inlet jet comes out of the shroud under the liquid thus avoiding entrainment of oxygen. The portion of the shroud kept submerged under the free surface is known as shroud immersion depth and that is normally controlled to get better mixing in a tundish. The second objective of the present computation is to study the effect of an APB, put under the inlet stream (Figure 1(c)), and the shroud immersion depth (Figure 1(d)) on mixing by using various turbulence models.

Before proceeding to compute the above, a detail computation on a single strand (exit) tundish is done with all the six turbulence models, which have been compared with the experimental measurement of Singh and Koria (1993). Experimental measurements and numerical computation for a multi exit tundish can be found from the work of Morales *et al.* (2000a, b) where, the authors have computed the mixed and the dead volume in a tundish fitted with a turbulence inhibitor and dam, but they have not shown the effect of various turbulence models on the optimum values of the height of the inhibitor or the placement of the dam so as to obtain highest mixing parameters such as the mixed or the dead volume or a ratio of the two.

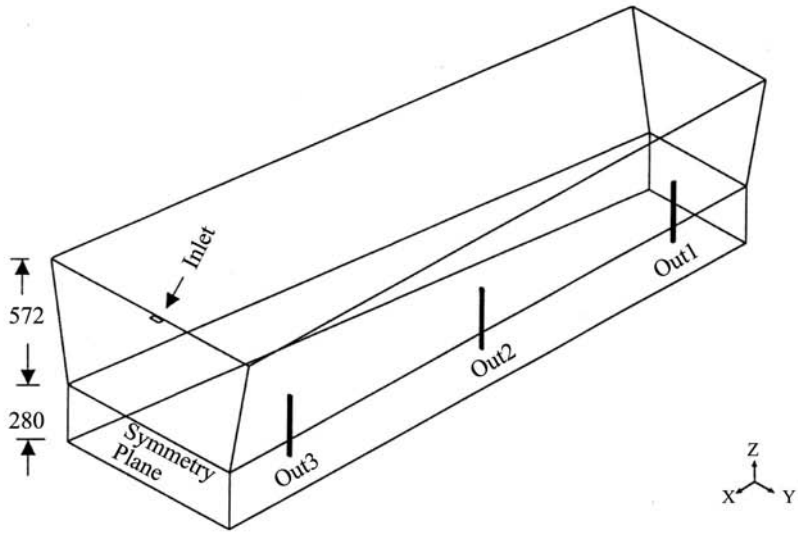

(a) Geometry of the six strand billet caster tundish about the symmetry plane with the inlets and outlets drilled through the bottom pad

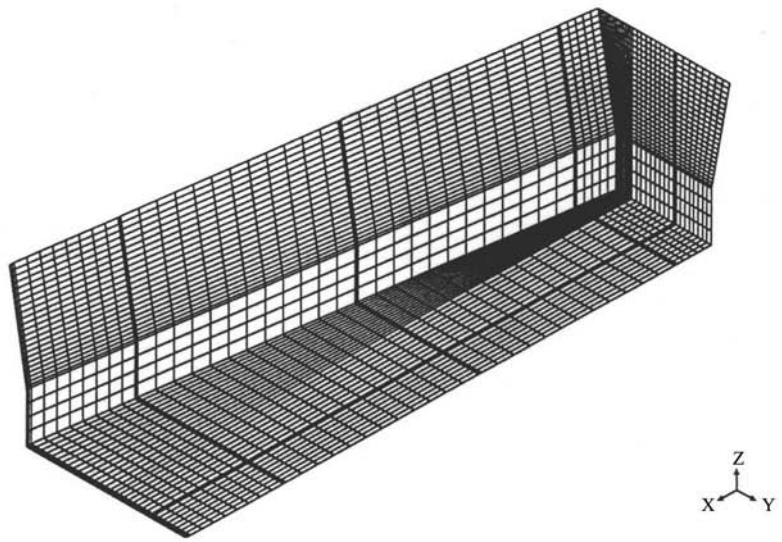

(b) The billet caster tundish with the boundary fitted grid lines shown on the outermost surfaces

(*Continued*)

Figure 1.

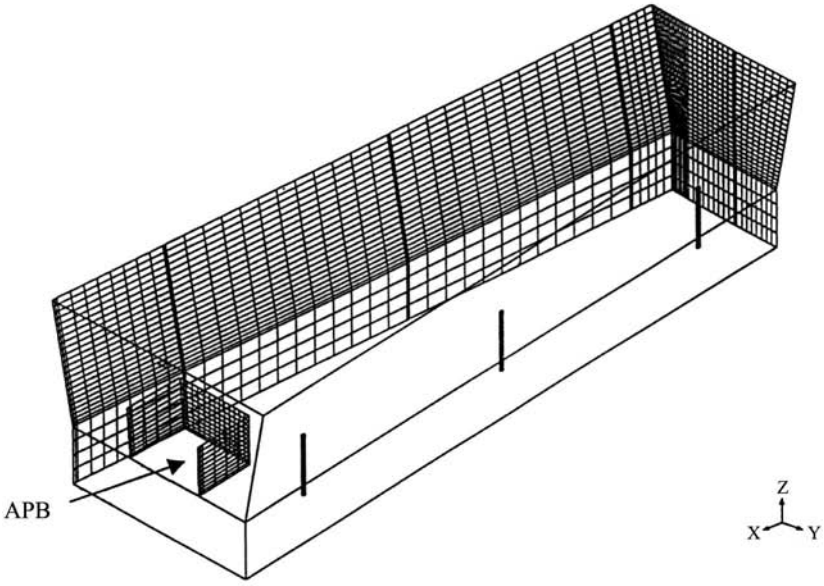

(c) Boundary fitted grid lines showing the outer surfaces along with the advance pouring box (APB) placed on the bottom plane of the tundish

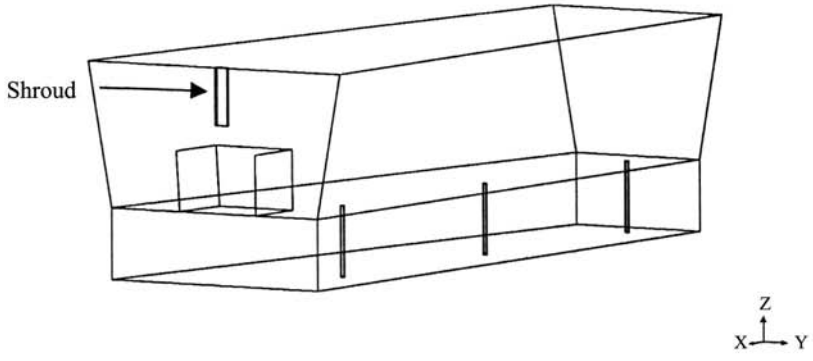

(d) Geometry of the tundish (about the symmetry plane) with the APB placed on the bottom plane along with the shroud

Figure 1.

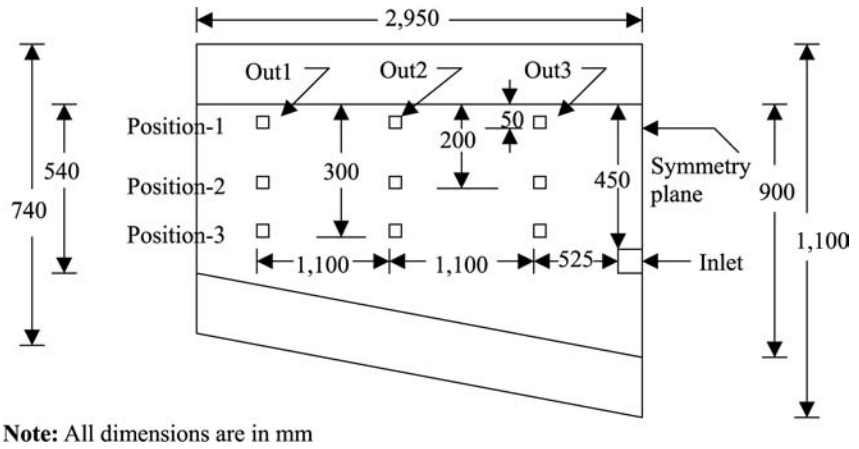

Figure 2.
Top view of the tundish about the symmetry plane with the location of the outlets at the bottom plane

Mathematical formulation and assumptions

The flow field in the tundish is computed by solving the mass and momentum conservation equations in a boundary fitted coordinate system along with a set of realistic boundary conditions. The tundish boundary does not conform to a regular Cartesian system because it is an inclined wall delta shape tundish, so the use of BFC was made to solve all the conservation equations. The species continuity equation is solved in a temporal manner to capture the local variation of the concentration of the dye in the tundish. The free surface of the liquid in the tundish was considered to be flat and the slag depth was considered to be insignificant. With these two assumptions the flow field was solved with the help of the following equations (in tensorial form) with six turbulence models (k-ε, k-ε-RNG, low Re k-ε Lam-Bremhorst, CK, CKL and the CEV model). Isothermal flow conditions have been modeled in the present study just to understand the effect of pertinent geometrical parameters on the performance of the tundish.

In actual practice the flow within the tundish is never steady even if it is running full for a long time. When the tundish goes for a grade change or ladle change the flow really becomes transient and then slowly approaches towards steady-state, but is never steady in a true sense. So to this extent it can be said that the flow behavior inside a tundish is rather unstable and none of the turbulence models cited above can be expected to predict the flow behavior exactly. Rather all the turbulence models predict an average mode of performance through the use of the eddy viscosity conception that has been built in them and they average out the stochastic variations caused by turbulence within the system unless a full stress model is used which again is a very time-consuming job because of the six extra partial differential equations which need to be solved. However, for an industrial application with a complicated geometry like the delta shape tundish of the present situation it is a good idea to use all the available turbulence models for obtaining predictions as well as comparisons of the turbulence models so far as the optimum values are concerned, which has been the main objective this paper.

Governing equations
Continuity

$$\frac{\partial}{\partial x_i}(\rho U_i) = 0 \tag{1}$$

Momentum

$$\frac{\mathrm{D}(\rho U_i)}{\mathrm{D}t} = -\frac{\partial p}{\partial x_i} + \frac{\partial}{\partial x_j}\left[\mu\left\{\frac{\partial U_i}{\partial x_j} + \frac{\partial U_j}{\partial x_i}\right\} - \overline{\rho u_i u_j}\right] \tag{2}$$

Turbulent kinetic energy

$$\frac{\mathrm{D}(\rho k)}{\mathrm{D}t} = D_k + \rho P - \rho\varepsilon \tag{3}$$

Rate of dissipation of k

$$\frac{\mathrm{D}(\rho\varepsilon)}{\mathrm{D}t} = D_\varepsilon + C_1^* f_1 \rho P \frac{\varepsilon}{k} - C_2^* f_2 \frac{\rho\varepsilon^2}{k} \tag{4}$$

Concentration

$$\frac{\partial}{\partial t}(\rho C) + \frac{\partial}{\partial x_i}(\rho u_i C) = \frac{\partial}{\partial x_i}\left(\frac{\mu_{\mathrm{eff}}}{\sigma_{\mathrm{c}}}\frac{\partial C}{\partial x_i}\right) \tag{5}$$

where

$$\overline{u_i u_j} = \frac{2}{3}k\delta_{ij} - \nu_{\mathrm{t}}\left(\frac{\partial U_i}{\partial x_j} + \frac{\partial U_j}{\partial x_i}\right)$$

$$\nu_{\mathrm{t}} = C_\mu f_\mu k^2/\varepsilon, \quad \mu_{\mathrm{eff}} = \rho\nu_{\mathrm{t}} + \mu$$

$$D_\phi = \frac{\partial}{\partial x_j}\left[\left(\mu + \frac{\mu_{\mathrm{t}}}{\sigma_\phi}\right)\frac{\partial\phi}{\partial x_j}\right], \quad P = -\overline{u_i u_j}\frac{\partial U_i}{\partial x_j}$$

Constants used in different turbulence models are as follows

k-ε model

$$C_1^* = C_1 = 1.44, \quad C_2^* = C_2 = 1.92, \quad \sigma_{\mathrm{c}} = 1.0$$

$$\sigma_k = 1.0, \quad \sigma_\varepsilon = 1.3, \quad f_1 = f_2 = f_\mu = 1, \quad C_\mu = 0.09$$

RNG model

$$C_2^* = C_2 + \frac{C_\mu \eta^3(1 - \eta/C_4)}{1 + C_5\eta^3},$$

$$\eta = Sk/\varepsilon, \quad S = \sqrt{2S_{ij}S_{ij}} = \text{modulus of the mean rate-of-strain tensor}$$

$$S_{ij} = \frac{1}{2}\left(\frac{\partial U_i}{\partial x_j} + \frac{\partial U_j}{\partial x_i}\right)$$

$$C_1^* = C_1 = 1.42, \quad C_2 = 1.68, \quad C_4 = 4.38, \quad C_5 = 0.012, \quad C_\mu = 0.085$$

$$\sigma_c = 1.0, \quad \sigma_k = 1.0, \quad \sigma_\varepsilon = 1.3, \quad f_1 = f_2 = f_\mu = 1$$

Lam-Bremhorst model

$$f_\mu = [1 - e^{(-0.0165\,\mathrm{Re_n})}]^2\left(1 + \frac{20.5}{\mathrm{Re_t}}\right), \quad f_1 = 1 + \left(\frac{0.05}{f_\mu}\right)^3$$

$$f_2 = 1 - \exp(-\mathrm{Re_t^2}), \quad \mathrm{Re_n} = \frac{\sqrt{k}Y_n}{\nu}, \quad \mathrm{Re_t} = \frac{k^2}{\nu\varepsilon}$$

Y_n=Distance to the nearest wall

$$C_1^* = C_1 = 1.44, \quad C_2^* = C_2 = 1.92, \quad \sigma_c = 1.0, \quad \sigma_k = 1.0, \sigma_\varepsilon = 1.3, \quad C_\mu = 0.09$$

Chen-Kim model

$$C_1^* = C_1 + C_3\frac{P}{\varepsilon}, \quad C_1 = 1.15, \quad C_3 = 0.25, \quad C_2^* = C_2 = 1.9, \quad \sigma_c = 1.0$$

$$\sigma_k = 0.75, \quad \sigma_\varepsilon = 1.3, \quad f_1 = f_2 = f_\mu = 1, \quad C_\mu = 0.09$$

CKL model

$$f_\mu = [1 - e^{(-0.0165\,\mathrm{Re_n})}]^2\left(1 + \frac{20.5}{\mathrm{Re_t}}\right), \quad f_1 = 1 + (0.05/f_\mu)^3$$

$$f_2 = 1 - \exp(-\mathrm{Re_t^2}), \quad \mathrm{Re_n} = \frac{\sqrt{k}Y_n}{\nu}, \quad \mathrm{Re_t} = \frac{k^2}{\nu\varepsilon}$$

Y_n = distance to the nearest wall

$$C_1^* = C_1 + C_3\frac{P}{\varepsilon}, \quad C_1 = 1.15, \quad C_3 = 0.25, \quad C_2^* = C_2 = 1.9, \quad \sigma_c = 1.0$$

$$\sigma_k = 0.75, \quad \sigma_\varepsilon = 1.3, \quad C_\mu = 0.09$$

CEV model

k and ε equations are not solved. μ in the momentum equation (equation (2)) is replaced by

$$\mu_{\mathrm{eff}} = 200 \times \mu_{\mathrm{laminar}}$$

The Reynolds stress term is discarded in equation (2).

Computation of mixed and dead volume (Jha and Dash, 2002; Levenspiel, 1972; Szekely and Themelis, 1971)

$$\text{Theoretical residence time } \tau = \text{volume of tundish}/(\text{volumetric flow rate}) \quad (6)$$

$$\text{Actual residence time } t_r = \frac{\sum C_{av_i} t_i}{\sum C_{av_i}}, \quad i = 1, 2, 3 \quad \text{(for the three outlets)}, \quad (7)$$

In equation (7) the integration is carried over a time span of 2τ with an equal interval of time step.

$$\text{Average break through time, } t_p = \text{First appearance of tracer at the exits (time to be averaged for multi exits)} \quad (8)$$

In case of a multi strand tundish, the value of t_p will vary from one outlet to the other. The tracer will appear suddenly at the outlet, which is placed nearest to the inlet. So the value of t_p will be very small for this outlet whereas for other outlets t_p will have a higher value. In order to model the break through time for the entire tundish, the individual values of t_p for all the outlets are added and an average value of t_p is taken to compute the plug volume. The dead volume is computed from equation (9) after computing the theoretical and actual mean residence time from equations (6) and (7), respectively. The mixed volume is computed from equation (11) after the dead and plug volumes are computed.

$$\text{Fraction of dead volume, } V_d/V = 1 - t_r/\tau \quad (9)$$

$$\text{Fraction of plug volume, } V_p/V = t_p/\tau \quad (10)$$

$$\text{Fraction of mixed volume, } V_m/V = 1 - V_p/V - V_d/V \quad (11)$$

Boundary conditions

Boundary conditions can be well visualized with reference to Figure 1(a) and (c). The symmetry plane is given a symmetry boundary condition, which implies a zero gradient condition for all variables normal to that plane. The walls were set to a no slip condition and the turbulent quantities were set from a log law wall function for the k-ε and k-ε-RNG and the CK models. The following "logarithmic law of the wall" (Ferziger and Peric, 1999) was utilized to compute the value of $k(k_p)$ and $\varepsilon(\varepsilon_p)$ at the first cell in contact with the wall by considering the production and dissipation of turbulent quantities to be in local equilibrium near the wall.

$$\frac{\rho u_p k_p^{1/2} C_\mu^{1/4}}{\tau_W} = \frac{1}{\kappa} \ln(Ez^+),$$

where

$$z^+ = \frac{z_p k_p^{1/2} C_\mu^{1/4}}{\nu}, \quad E = 8.6 \quad \text{and} \quad \kappa = 0.41$$

$$\varepsilon_{\mathrm{p}} = \frac{C_{\mu}^{3/4} k_{\mathrm{p}}^{3/2}}{\kappa z_{\mathrm{p}}}$$

The same wall function is used in the k-ε-RNG and the CK model for the computation of the near wall turbulent quantities. It can be noticed from the above equation that the first node distance from the wall, z_{p} influences the near wall turbulent quantities. The influence of z_{p} on the mixing parameters (V_{m}/V, V_{p}/V and V_{d}/V) has been studied by Jha and Dash (2002) in an earlier computation in order to arrive at a suitable grid distribution near the wall which can predict more accurate results for mixing. The grid distribution from the earlier computation has been adopted here for better accuracy of the result.

For the Lam-Bremhorst model and the CKL Re model $k = 0$ and a normal gradient of ε to the wall was set to 0. At the inlet, the velocity of the incoming jet was set to a prescribed value of 1.4 m/s (1.61 ton/min of liquid steel) with a turbulent intensity of 2 percent. The intensity of turbulence defined here is $I = \sqrt{\overline{w^2}}/w_{\mathrm{inlet}}$ from which the value of k at the inlet can be prescribed as $k = 0.5(I \times w_{\mathrm{inlet}})^2$. The value of ε at the inlet is computed from the relation

$$\varepsilon_{\mathrm{inlet}} = \frac{C_{\mu}^{3/4} k_{\mathrm{inlet}}^{3/2}}{0.1H},$$

where H is the hydraulic radius of the inlet pipe (Launder and Spalding, 1972).

The top surface of the tundish was taken to be a free surface where a zero shear stress condition was applied according to Illegbusi and Szekely (1989), Szekely *et al.* (1987) and Tacke and Ludwig (1987). The bottom of the tundish was treated like a wall where no slip conditions were used for the velocity. At the outlets a fixed pressure of 0 Pa (relative to the ambient) was applied.

Mass transfer boundary and initial conditions

The wall of the tundish was considered to be impervious to the dye, so a zero gradient condition for the dye was used on the walls. At the outlet and at the free surface also zero gradient conditions were used for the dye (Illegbusi and Szekely, 1988, 1989). At the symmetry plane zero gradient condition for the dye was also used. Initially at $t = 0$ s, the concentration of the tracer everywhere in the tundish was assumed to be zero excluding the length of the shroud submerged below the free surface of the liquid in the tundish in which part the concentration was assumed to be 1. At the inlet to the shroud (or at the inlet when there is no shroud or when the shroud length is zero) the concentration of the dye was prescribed to be 1 from 0 to 5 s after which the concentration was kept at zero. When the shroud had a definite length the concentration inside the shroud was assumed to be one for the first 5 s and subsequently, it was set to zero. This means the concentration inside the shroud was not computed (similar approach can be found in the work of Morales *et al.* (2000b)) rather it was assumed that the liquid inside the shroud was perfectly mixed and the concentration at the shroud exit (nozzle tip) is same as that at the inlet. The computation of the tracer concentration inside the shroud would need fine grid and much smaller time step, which will elongate the overall computational time and eventually will not make much of a difference to the overall computation of mixed and dead volume because the shroud volume is too small compared to the entire volume of the tundish. So it is a good idea to assume the concentration inside the shroud to be

1(which is most likely uniform for a short time of 5 s) and avoid its computation. Five seconds is normally very short compared to the mean residence time of the tundish, so the influx of the dye during its travel is not likely to change the local velocity field in the tundish as the mass influx of the dye is also very small (Szekely and Themelis, 1971).

Method of solution

The set of partial differential equations (1)-(5) was solved with the help of the above boundary conditions numerically in a finite volume technique using the educational version of the CFD software Phoenics. The partial differential equations were integrated over a control volume to find out the fluxes (of mass and momentum as well as that of the dye) through all the faces, and the flux balance is made over all the control volumes, which yield a set of linear algebraic equations. The set of algebraic equations is solved by the tri-diagonal matrix (TDM) method for momentum and by a whole field solver, taking one from the family of conjugate gradients for the pressure correction equation. The species continuity equation is solved at each and every time step using the TDM matrix method once the steady-state solution for the momentum equations is obtained. The solutions are said to have converged when the whole field normalized residuals for each of the velocity components and mass fall below unity. A false time step relaxation of 0.5 was used for all the variables for faster convergence. Control volumes (CV) of $66 \times 27 \times 30$ ($X \times Y \times Z$) were used for the computation of the single strand bare tundish for all the high RE k-ε models and the CEV model. By changing the control volumes to $76 \times 37 \times 40$, it was observed that the changes in the mixed and dead volumes were less than 0.2 percent. For the Lam-Bremhorst model and the Chen-Kim Low Re model control volumes of $80 \times 42 \times 38$ ($X \times Y \times Z$) were used which could yield a $z+$ value of nearly 1 or somewhere less than 1 near the tundish wall. Increasing the CVs by another 10 in all directions did not improve the mixed volume and the mean residence time, even by 0.1 percent. Grid density near the walls was kept higher for all the high Re number models so that the near wall $z+$ could lie between 30 and 50. Grids were put closer towards the outlets and towards the wall of the APB (not shown in Figure 2) so that the turbulence diffusion as well as the variation in the velocity field could be caught accurately. Near the point of impact of the jet (inside the APB) grids were also made finer so that artificial diffusion arising due to first order upwind scheme could be kept lower. Grids towards the top flat portion of the tundish (where a symmetry condition is prescribed) can be spaced more widely because the variation in all the flow quantities near this zone is going to be low compared to the bottom of the tundish where grid density was made higher. From the temporal variation of concentration the actual mean residence time and all other times was found out by simple integration (equation (7)) after which the ratio of mixed to dead volume could be found out. For the computation, the density of liquid steel was taken to be 7,100 kg/m^3 all through the volume and the kinematic viscosity (Illegbusi and Szekely, 1988; Mazumdar and Guthrie, 1999) to be 0.913×10^{-6} m^2/s.

Results and discussions

The flow field in the six strand (multi exit) tundish was obtained by solving the Navier-Stokes equations numerically and then the tracer dispersion was computed by injecting some dye into the inlet. From the tracer dispersion curve the mixed volume and the dead volume were computed as per equations (9)-(11). The analysis of mixing

was done with respect to the ratio of mixed to dead volume for different geometrical positions of the outlet, different height of the APB and different shroud immersion depth by using six different turbulence models. The mixed and dead volumes are direct indices of mixing in a tundish. If the mixed volume is large that means more of the tundish volume is utilized in mixing the fluid. Similarly, it can be said that if the dead volume is low then most of the volume of the tundish is utilized by the fluid for mixing. So a ratio of mix to dead volume (Singh and Koria, 1995) and the mean residence time are better parameters to describe the mixing in a tundish as a function of other geometrical parameters. In the present study, the effect of outlet positions, height of APB and the shroud immersion depth on mixing has been carried out. We will discuss the variation of the mean residence time and the ratio of mixed to dead volume (V_m/V_d) as a function of outlet positions, height of APB and shroud immersion depth. The temporal variation of the tracer concentration at the outlets for all the respective cases is not discussed here.

Validation with experiment

Singh and Koria (1993) have done the experiment for a single inlet-single outlet tundish in which they have measured the tracer concentration with time at the outlet. The geometry of their tundish and the computational cells used for the computation are shown in the work of Jha and Dash (2002). In their experiment the bath height was kept at 260 mm and accordingly the same height was used for the computation where the free surface boundary condition was applied. Figure 3(a) and (b) show the temporal variation of the tracer concentration (non-dimensional) with non-dimensional time and a comparison of the present numerical computation with all the six turbulence models with that of the experiment. It can be seen from the figure that the tracer concentration has two peaks in the experiment (one at $t = 0.15$ and the other at $t = 0.42$) and four of the six turbulence models (k-ε, k-ε-RNG, Lam-Bremhorst and CK) are able to predict both peaks, but they have their own delays in time while predicting them. The other two turbulence models namely, the CKL and the CEV model are not able to predict both peaks and they only show a single peak, but the peak value predicted by the CEV and the CKL models are very close to the second peak of the experiment.

When the tracer is first added at the inlet it moves with the flow field towards the outlet due to the steady velocity field present in the tundish. It takes little time to reach the outlet and that can be seen clearly in Figure 3(a) and (b) when the concentration just starts to rise from a value of zero. The concentration at the outlet then increases with time due to plug flow present in the tundish. A sharp increase in the tracer concentration shows that mixing has not taken place in the tundish because the tracer that has been added has just found its way to the outlet for which there is a sudden jump in the concentration at the outlet. If there were mixing then the change in the concentration at the outlet could be gradual, which is seen to be happening at a later time ($t > 0.5$). However after the initial peak, the tracer concentration falls suddenly and then gradually increases to another peak after which it slowly decreases with time. This happens because after the sudden release of tracer material at the outlet there is no tracer present around the outlet for which the concentration suddenly falls. However after a while the fluid brings in some more tracer, which has the chance to be mixed by the rebounded fluid from the wall for which the concentration again increases and attains a peak value. This time the tracer concentration does not increase as suddenly

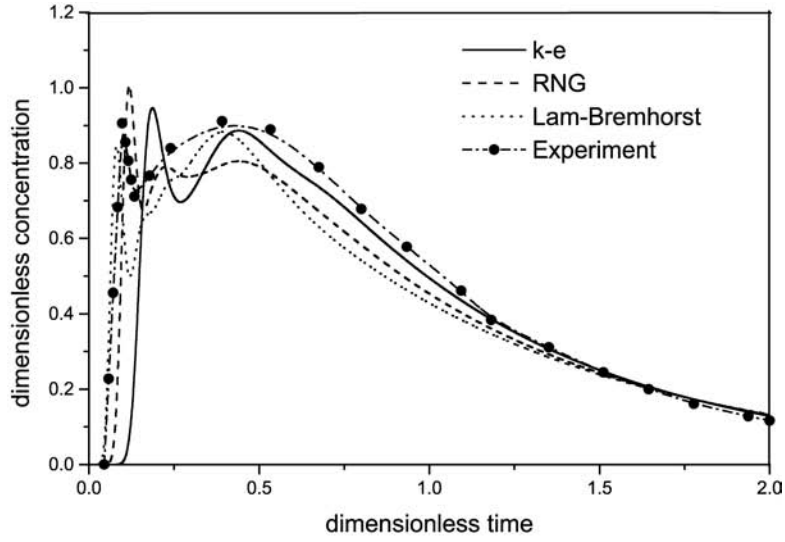

(a)

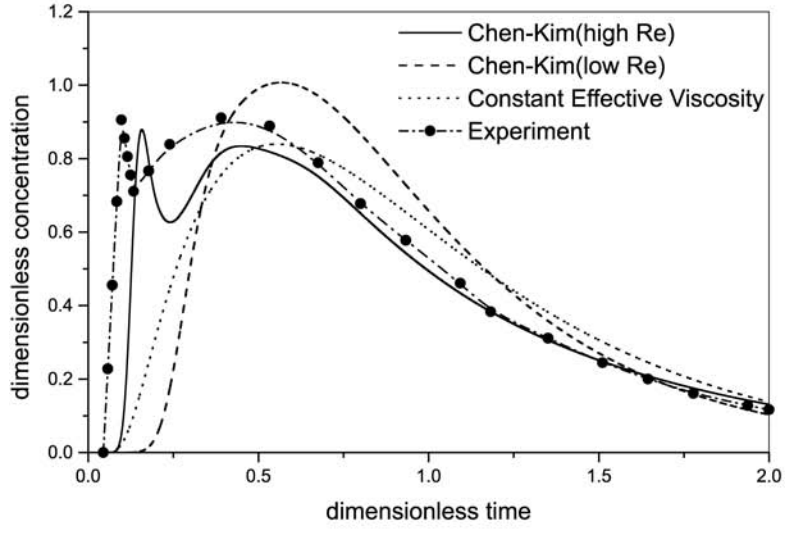

(b)

Figure 3.
Temporal variation of tracer concentration at the outlet of a single strand tundish: a comparison between experiment and various turbulence models

as it does the first time. After the second peak the tracer slowly goes out of the system for which the concentration slowly falls with time and after about three times the mean residence time, the concentration falls to nearly zero. So it can be found from this experimental observation that mixing has really taken place after a non-dimensional time of 0.2 from when the rise in tracer concentration has become gradual as well as its fall.

It can be seen that the initial rise in the tracer concentration is well predicted by the Lam-Bremhorst model as well as the first peak. Also the k-ε RNG model is capable of predicting the initial rise well, along with the prediction of the first peak. But the standard high Reynolds number k-ε model and the CK model show a delay in predicting the first tracer appearance although it predicts the magnitude of the first peak value well compared with the other two models. In the k-ε model and the Chen-Kim model, it has been observed that the value of k remains high all through the flow field compared with the other four models. Hence, the turbulent diffusion remains high, as a result mixing becomes high and the tracer appears late at the outlet. In the RNG model the extra source term in the dissipation equation (4) increases the rate of dissipation near the wall and causes the turbulent kinetic energy to remain low for which the turbulent diffusion remains low causing mixing to be relatively low in comparison with the standard k-ε model. The same effect also comes through the low Reynolds number Lam-Bremhorst model where the overall value of turbulent kinetic energy in the vicinity of wall remains low, causing turbulent diffusion of the tracer concentration to be low. So the RNG and the Lam-Bremhorst model predict the first appearance of tracer to be quicker than the k-ε and the Chen-Kim model. However, after $t > 0.5$ the k-ε model and the Chen-Kim model predict a better match in concentration with time compared with the other four models simply because the k-ε models produce more turbulent kinetic energy, which aids diffusional mixing better than the other four models. After a time of 1.5 all the six turbulence models predict the same concentration with time. The CEV model was employed with a turbulent viscosity of 200 times the laminar viscosity. This helps very high turbulent mixing of the tracer so the first appearance of tracer at the outlet (Figure 3(b)) is delayed very much. However, after a time of about 0.4 the tracer concentration predicted by this model is close to the experimental observation. The CKL model however, becomes over diffusive taking the same Lam-Bremhorst wall damping functions along with an extra source term present in equation (4) and this behaves similarly like the constant effective viscosity model.

Table I shows a comparison of the bulk flow properties for the tundish with all the six turbulence models. It can be seen from the table that the mean residence time as well as V_m/V_d are well predicted by the k-ε model ($z_p = 8.67$ mm) and also by k-ε

Table I.
A comparison of the bulk flow properties obtained from various turbulence models with the experiment

Properties used for comparison	Experiment of Singh and Koria (1993)	k-ε	k-ε RNG	k-ε Lam-Bremhorst	k-ε Chen-Kim	CKL	CEV
V_m	74.29	69.25	70.33	71.4	70.97	69.43	79.21
V_d	20.14	20.5	23.38	24.82	20.4	13.49	12.16
V_p	5.57	10.25	6.29	3.78	8.63	17.08	8.63
t_r (s)	444	442	426	418	442.56	481	488.38
V_m/V_d	3.689	3.378	3.008	2.876	3.479	5.147	6.514

Chen-Kim model. These values are favorably compared with the experimental measurement. The mixed volume (percent volume of the entire tundish) is under-predicted by the k-ε model where as RNG and Lam-Bremhorst model predict the mixed volume closer to the experiment while in case of dead volume, k-ε as well as k-ε Chen-Kim model predict closer to experimental value as compared with the over predicted value by the RNG and the Lam-Bremhorst model. It can be concluded from Table I that the k-ε model as well as its Chen-Kim version are well capable of predicting the mean residence time and V_m/V_d closer to the experimental observation in a bare tundish although the flow field inside a tundish is highly recirculating. Although the k-ε model does not predict the variation of temporal concentration well at the beginning, the initial mismatch in concentration with the experimental observation does not influence the prediction in mean residence time because the mean residence time is found out by taking the area moment about the concentration axis. So the initial mismatch does not count much in the overall integration, whereas the matching with experimental observation after the initial transience counts much towards predicting the mean residence time. Although the Lam-Bremhorst model predicts the concentration well at the beginning, it does not do that well towards the later part, so the prediction in mean residence time suffers a little when compared with the experimental observation. The CKL model and the constant effective viscosity model are over diffusive due to which they aid excessive diffusional turbulent mixing as a result the mean residence time and V_m/V_d are over predicted by these two models.

Effect of outlet positions on V_m/V_d and mean residence time

Figure 4(a) shows the variation of mean residence time and Figure 4(b) the variation of V_m/V_d when the distance of the outlets from the wall is changing. When the distance of the outlets is increased from the wall the mean residence time and V_m/V_d both attain a peak and then they decrease with the increasing distance of the outlets from the wall. This happens with three of the turbulence models (k-ε, k-ε-RNG and the Lam-Bremhorst). The other three models namely: Chen-Kim, CKL and the CEV, do not predict this trend. The CEV model shows a sharp increase in the mean residence time and V_m/V_d as the distances of the outlets from the wall increase. The CK and CKL model show a very marginal decrease in the mean residence time and V_m/V_d as the distances of the outlets increase from the wall.

When the outlets are 200 mm away from the wall V_m/V_d attains a peak value (as per k-ε, k-ε-RNG and the Lam-Bremhorst) signifying best possible mixing in the tundish. When the outlets move still further away from the wall, V_m/V_d decreases because the tracer before dispersing any further finds its way directly to the outlet for the discharge. Thus, it can be said that there exists an optimum location for the outlets where best possible mixing can be achieved. Three turbulence models out of the six used for the simulation predict outlet position-2 as the optimum location. The variation of mean residence time is also a direct indication of mixing in a tundish. From Figure 4(a) it is seen that the outlet position-2 has the highest mean residence time, hence mixing in the tundish can be better if the outlets are placed at this position.

It can be seen that the RNG and the k-ε model almost predict V_m/V_d very close to each other (with a maximum of 6 percent deviation from k-ε model) while the Lam-Bremhorst model predicts with a maximum difference of 12 percent from the k-ε model. However, all three models show the same trend in predicting V_m/V_d

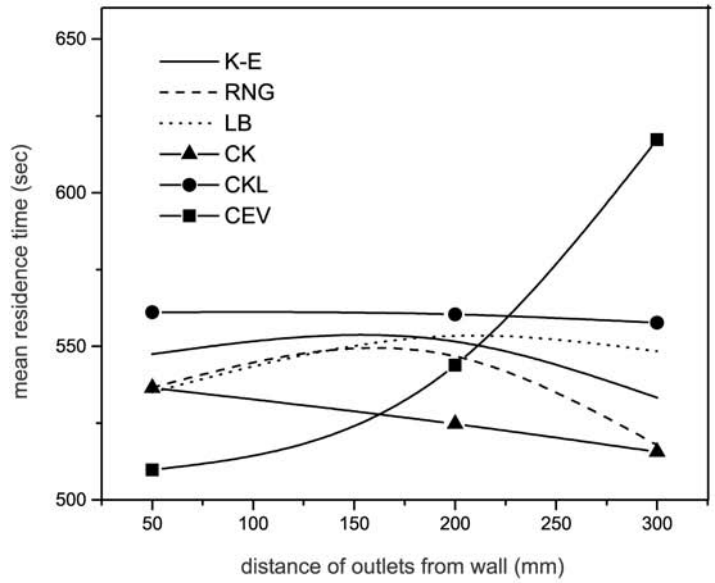

(a) Variation of mean residence time with outlet positions using different turbulence models

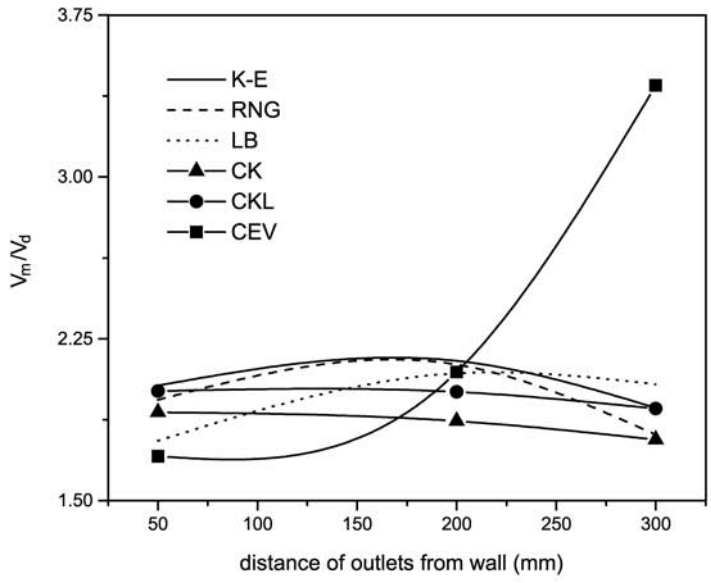

(b) Variation of V_m/V_d with outlet positions using different turbulence models

Figure 4.

and the mean residence time. In the prediction of mean residence time all the three turbulence models are close to each other with a maximum relative difference of 5 percent existing between the RNG and the Lam-Bremhorst model.

Effect of the height of APB

It is found out from the previous section that there probably exists an optimum location for the outlets where mixing is best achieved in a tundish. Taking outlet position-2 as the optimum location, an APB was put on the bottom of the tundish which could surround the striking inlet jet very easily. The APB stops the spreading jet on the bottom of the tundish and redirects the flow towards the top free surface of the tundish. The flow rises from within the APB as a plume and then disperses outside the APB into the tundish and thus, helps better mixing (please see vector plot in Jha *et al.* (2001)). If the height of the APB is made to change (the base area remaining same) then the rising plume from within the APB can rise to the level of the top free surface and can disperse at the top free surface. The question is, whether the dispersion at the top free surface can induce a better global mixing in the tundish or the dispersion of the rising jet should take place somewhere below the top free surface? This has been addressed in the present computation by making a simulation where the height of the APB is changing from 0 to 350 mm (the top free surface is located at 572 mm).

Figure 5(a) and (b) shows the variation of mean residence time and V_m/V_d as a function of the height of APB with six turbulence models, respectively. It can be seen that the k-ε and the CKL model predict a distinct peak in the mean residence time as well as in V_m/V_d as the height of the APB is increasing from 0 to 350 mm. This peak is attained at an APB height of 210 mm. The Lam Bremhorst and the RNG model show a very marginal change in the mean residence time with the increase of the height of APB. The CEV model shows a peak in the mean residence time and in the ratio of V_m/V_d when the height of the APB is 90 mm. The Chen-Kim model shows a monotonic rise in the mean residence time and V_m/V_d as the height of the APB increases.

An APB height of 0 mm, signifies the presence of no APB. The inlet jet after striking the bottom of the tundish spreads on it towards the outlets, failing to induce stronger mixing. But when the height of the APB has a finite value the rising plume from within the APB comes up to a certain distance towards the top free surface before its dispersion into the tundish. This helps better mixing because the rising plume sucks the surroundings fluid outside the APB and thus sets up a convection current around the APB which helps in mixing. So with the increase of the height of the APB the mean residence time as well as the ratio of mixed to dead volume V_m/V_d, are expected to rise and that is shown by at least two of the turbulence models. But when the height of the APB increases too much then the rising plume from within the APB reaches the top free surface of the tundish where it disperses on the free surface of the tundish without getting any chance to suck the surroundings fluid around the APB because the effective length of the rising plume has decreased as the APB height has increased. The plume, reaching the free surface, fails to induce a stronger circulation in the entire tundish because the surface area of the tundish is much larger and that offers almost no resistance to the flow of the plume on the free surface. So the global mixing will be poor if the height of the APB increases beyond a certain value. More details on

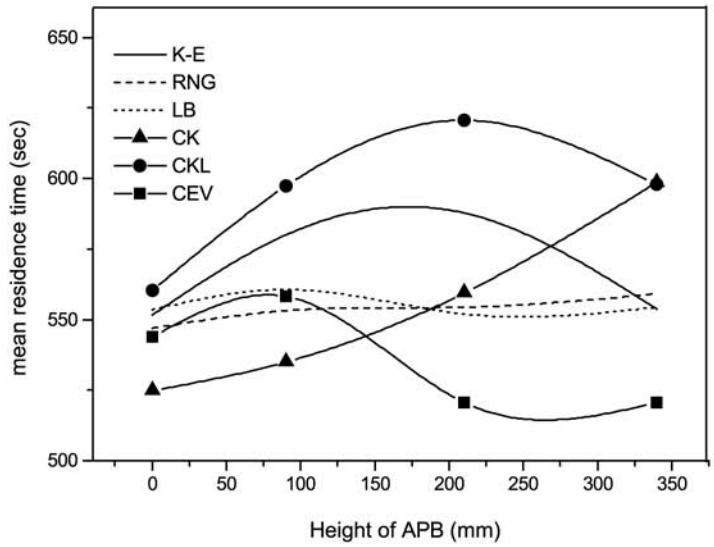

(a) Variation of mean residence time with Height of APB (outlets at position-2) using different turbulence models

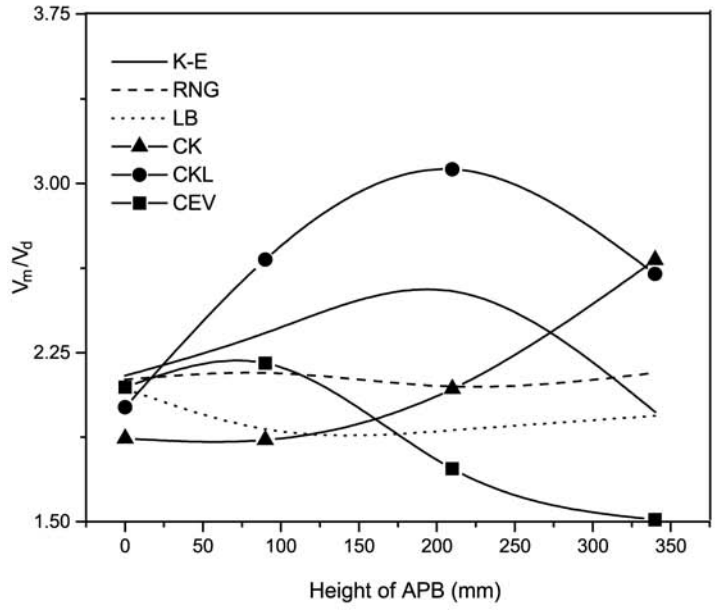

(b) Variation of V_m/V_d Height of APB (outlets at position-2) using different turbulence models

Figure 5.

this can be found in the work of Jha *et al.* (2001). Therefore, it is expected that there is a possibility of getting an optimum APB height where mixing can be better. This is shown in the present computation by at least two of the turbulence models.

Effect of the shroud immersion depth

It has been found out that there exists an optimum location of the outlets (position-2, 200 mm away from the inner wall) where mixing in the tundish is better and also at this optimum location there exists an optimum height of the APB (210 mm) which induces still better mixing. But for all these findings the shroud immersion depth was kept at 0 mm measured from the top free surface. Such an arrangement tells that the liquid jet comes out of the shroud exactly touching the top free surface of the liquid. In practice such an arrangement is normally avoided because the liquid jet will entrain the atmospheric oxygen with it which will be slowly dissolved in the steel later on. So normally the shroud is kept immersed under the free surface of the liquid. Hence the out coming jet from the shroud tip cannot entrain oxygen rather that will entrain the surroundings fluid in its vicinity which will help in better mixing of the fluid in the entire tundish. Then one becomes naturally curious to know to what depth the shroud should be immersed so as to get best possible mixing. This has been addressed here by making a simulation where the shroud immersion depth varies from 0 to 400 mm. The outlets are placed at position-2 and the height of the APB is fixed at 210 mm and then the simulation for the shroud immersion depth is carried on.

Figure 6(a) and (b) shows the variation of mean residence time and V_m/V_d respectively, as the shroud immersion depth varies from 0 to 400 mm by using six different turbulence models. It can be seen from the figure that all the turbulence models show different peak values in mean residence time and V_m/V_d as a function of the shroud immersion depth and there exists local maximum and minimum in five of the six turbulence models excepting the constant effective viscosity model which shows a maximum value in the mean residence time and V_m/V_d at a shroud immersion depth of 300 mm. But a careful examination of the curves depict that the k-ε model and the Lam-Bremhorst model along with the CEV model show a maximum in mean residence time and V_m/V_d at a shroud immersion depth of 300 mm also. The k-ε model and the CKL model show a minimum value in mean residence time and V_m/V_d at a shroud immersion depth of 100 mm whereas the CEV, Lam-Bremhorst and the RNG model show a rising value for these parameters. The Chen-Kim and RNG models show the highest value for mean residence time and V_m/V_d at a shroud immersion depth of 100 and 200 mm, respectively. It should be noted that while the k-ε, Lam-Bremhorst and the CEV models show locally maximum value for the mean residence time and V_m/V_d at a shroud immersion depth of 300 mm, but the RNG and the CKL model show locally minimum values for the same parameters at the same shroud immersion depth. The question now arises which shroud immersion depth is the optimum depth which can induce better mixing in the tundish when three (CKL, RNG, and CK) of the six turbulence models used show different optimum values in shroud immersion depth? We go for the other three turbulence models (k-ε, Lam-Bremhorst and CEV), which show peak values in the mean residence time and V_m/V_d consistently at a particular shroud immersion depth of 300 mm! This becomes the optimum shroud immersion depth where best possible mixing can be achieved. Naturally, such a decision becomes subjective in the absence of experimental observations. For most accurate prediction of

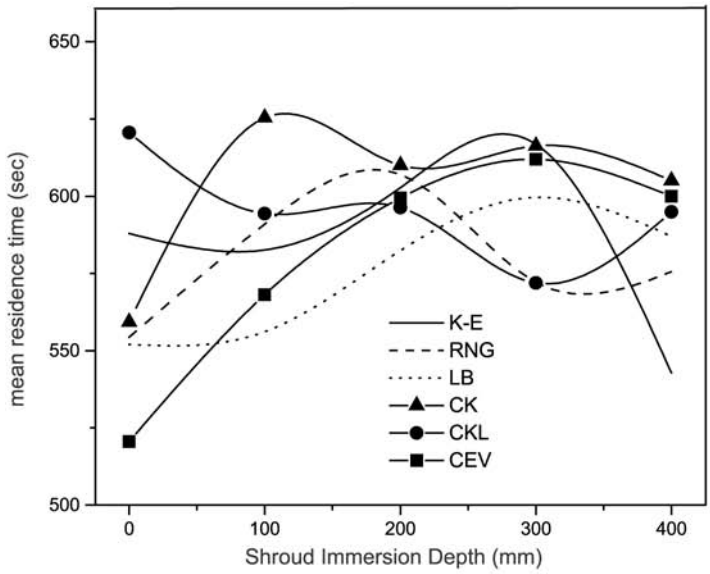

(a) Variation of mean residence time with Shroud Immersion Depth (outlets at position-2 with APB height = 240 mm) using different turbulence models

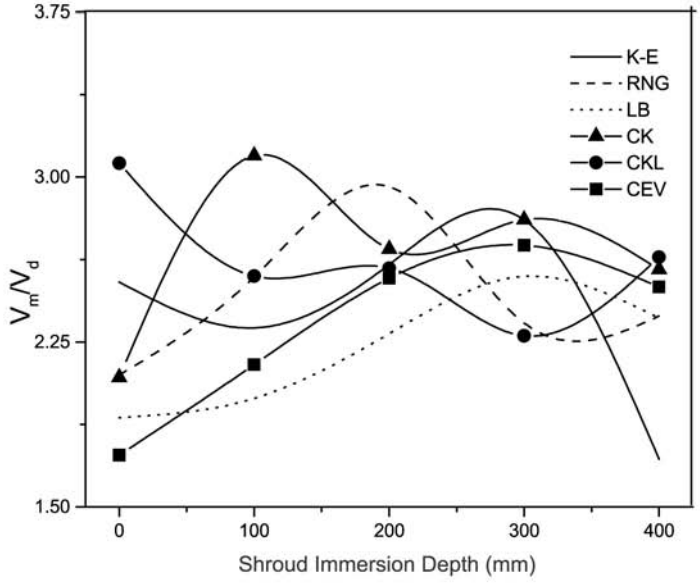

(b) Variation of V_m/V_d with Shroud Immersion Depth (outlets at position-2 with APB height = 240 mm) using different turbulence models

Figure 6.

the optimum value of shroud immersion depth it becomes mandatory that one has to perform the experiment before concluding anything from theory.

When the shroud immersion depth increases the liquid jet issued from the shroud tip is released at a higher depth from the free surface of the liquid. This decreases the entrainment of the surroundings liquid by the incoming jet, but the impact of the inlet jet on the bottom of the tundish becomes stronger as a result of the increasing shroud immersion depth. This jet creates a rising plume from within the APB, which becomes again stronger as the shroud immersion depth increases. The rising plume coming out of the APB sucks the surrounding liquid just around the APB, but the suction is in the opposite direction compared to the entrainment of the liquid created due to the incoming jet issued from the shroud tip. Owing to this opposing nature of flow in the vicinity of the shroud tip and the APB there exists an optimum shroud immersion depth for a particular height of the APB, which can induce maximum mixing in the tundish. If the suction created by the rising plume is stronger than the entrainment of the liquid created due to the incoming jet then the average velocity around the APB area remains higher for which the mixing becomes better (vector plot from Jha *et al.* (2001) for k-ε model can be referred). This is the reason why at a higher depth of the shroud the mixing increases. If the shroud immersion depth is increased from a value of 0 to about 100 mm the entrainment of the surroundings fluid due to the incoming jet suffers a loss because of a reduction in the effective length of the incoming stream, although the impact on the bottom rises a little, but the impact does not create a better suction for the rising plume. This is the reason why with the increase of the shroud immersion depth V_m/V_d and mean residence time can decrease. However, if the shroud immersion depth increases further the effective length of the incoming stream of jet decreases which further reduces the entrainment of the surroundings liquid but the rising plume from within the APB becomes stronger which again sucks the surroundings liquid, causing a stronger convection around the APB exit which helps mixing finally. So with the increase of the shroud immersion depth after a certain value the mean residence time and V_m/V_d can again increase. This explanation holds good for all other combinations of shroud immersion depth and APB height and naturally it can be expected that there will be local maximum and minimum in the mean residence time and V_m/V_d curve when plotted against the shroud immersion depth. This can be seen from Figure 4(a) and (b) how this phenomenon has been revealed by five of the six turbulence models used.

Effect of turbulent diffusion

The tracer dispersion is a transient phenomenon while the flow field has been computed to be steady. So the turbulent kinetic energy has a steady value and that differs from one model to the other. But the turbulent kinetic energy (k) plays a very important role in the dispersion of the tracer. If the value of k is high in a region that would help a quicker mixing of the tracer in that region and the dispersion of the tracer would be faster in that region. So if a model produces higher value of k near the bottom plane of the tundish then the tracer will be mixed better near the bottom plane and would get a chance to disperse easily to other region and hence may arrive late at the outlet because it spends time in mixing with other packets of fluids. On the other hand, if the value of k is lower then the mixing of the tracer will be poor and the tracer will get a chance to arrive at the outlet faster because it gets a straight path to the outlet.

It has no chance to be mixed with the other packets of fluid so it arrives straight at the outlet. This can be seen from Figure 3(a) and (b) how the different models behave as far as the tracer dispersion is concerned. The CKL model, which predicts much higher value of k compared to the k-ε or the RNG model has shown very late arrival of the tracer at the outlet (Figure 3(b)). Similar behavior can be seen from the CEV model where we have assumed the turbulent viscosity to be 200 times the laminar viscosity. Whereas for the k-ε, RNG and the Lam-Bremhorst model the predicted value of k is much lower than the CKL and the CEV model and these models predict quick arrival of the tracer at the outlet.

Figures 7(a)-(c), 8(a)-(c) and 9(a)-(c) show the field of k through their own contour plot for many different cases. From these figures the turbulent diffusion and convection can be compared in the tundish when the geometrical parameters changes. Figure 7(a) shows the plot of k when the outlet is at position-2, Figure 7(b) shows the plot of k when the APB height is 210 mm and Figure 7(c) shows the plot of k when the shroud immersion depth is 300 mm. It can be seen from the figure that the value of k is higher at the outlets (at all the three outlets) and higher at the point of impact (Figure 7(a)). The value of k is also higher within the APB (Figure 7(b)) and towards the top free surface and when the shroud immersion depth increases within the APB the value of k also rises towards the top free surface (Figure 7(c)). The plume rising from the APB can be seen to be having higher value of k. This phenomenon can be seen in the case of k-ε and the RNG model (Figure 8(a)-(c)). The rising plume of k from within the APB can be seen from Figures 7(b) and 8(b) and with a shroud immersion depth of 300 mm the rising plume can be seen from Figures 7(c) and 8(c). Both these models show almost the same behavior. The Lam-Bremhorst model however, predicts higher value of k near the outlet of the tundish, which can be seen from Figure 9(a)-(c). When the height of the APB is 210 mm the value of k within the APB remains high (Figure 9(b)) and when the shroud immersion depth increases to 300 mm the rising plume of k from the APB can be seen from the isolines of k shown in Figure 9(c).

Conclusions

The mass, momentum and the species conservation equations are solved numerically in a boundary fitted coordinate system comprising a typical industrial size tundish having a through put of 1.61 ton/min. The ratio of the mix to dead volume and the mean residence time are analyzed from the solution of the species conservation equation.

It is found that there exists an optimum location of the outlets where the ratio of the mix to dead volume and the mean residence time is the highest. Three of the six turbulence models (k-ε, k-ε RNG and k-ε Lam-Bremhorst) used for the simulation predict outlet position-2 as the optimum location.

At the optimum location of the outlets there exists an optimum APB height (of 210 mm) where the ratio of mix to dead volume and the mean residence time again attains a peak value signifying further enhanced mixing in the tundish. Two of the six turbulence models (k-ε and CKL) support this finding of 210 mm as the optimum height of the APB.

At the optimum location of the outlets and with an optimum height of the APB there exists an optimum shroud immersion depth where the ratio of mix to dead volume and the mean residence time further attains higher peak values signifying better mixing

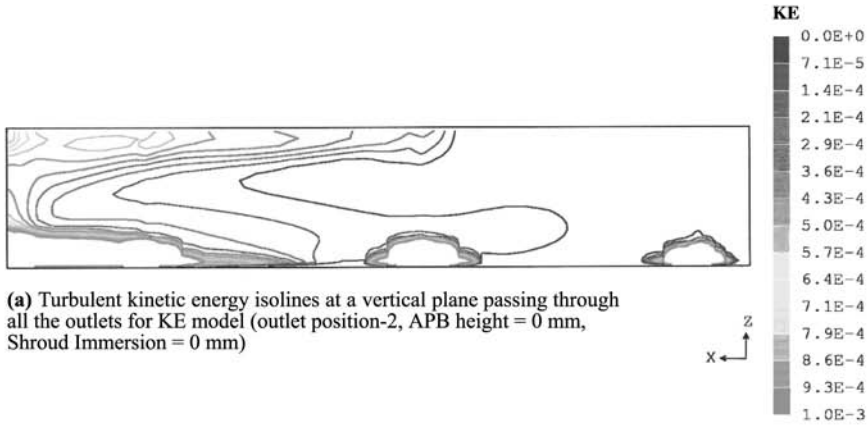

(a) Turbulent kinetic energy isolines at a vertical plane passing through all the outlets for KE model (outlet position-2, APB height = 0 mm, Shroud Immersion = 0 mm)

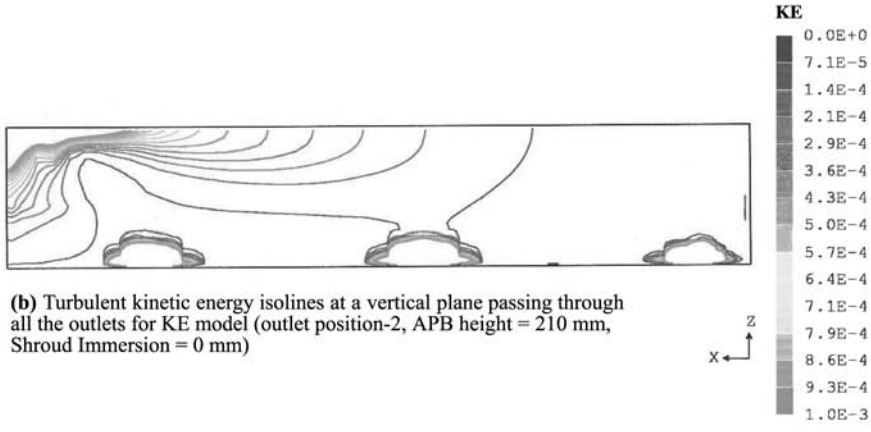

(b) Turbulent kinetic energy isolines at a vertical plane passing through all the outlets for KE model (outlet position-2, APB height = 210 mm, Shroud Immersion = 0 mm)

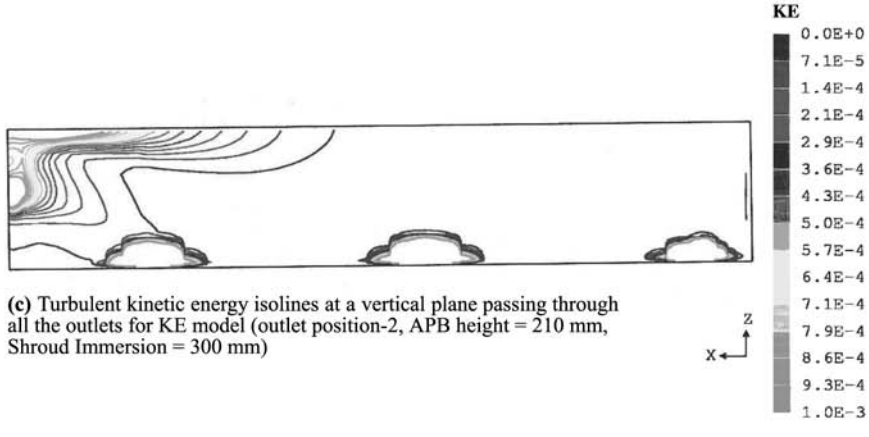

(c) Turbulent kinetic energy isolines at a vertical plane passing through all the outlets for KE model (outlet position-2, APB height = 210 mm, Shroud Immersion = 300 mm)

Figure 7.

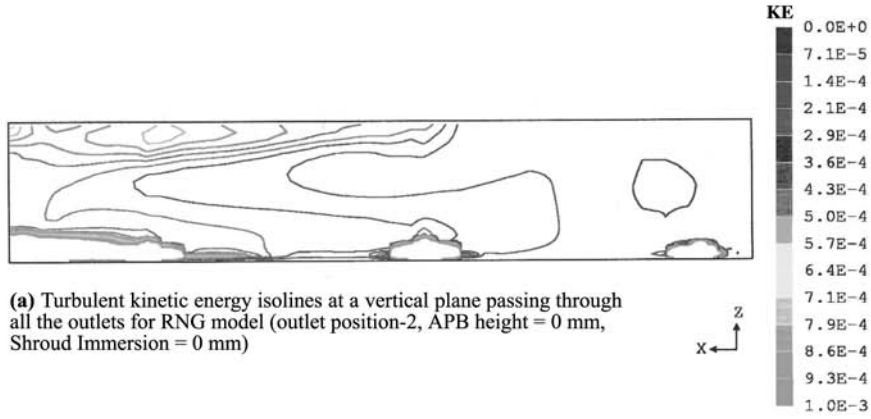

(a) Turbulent kinetic energy isolines at a vertical plane passing through all the outlets for RNG model (outlet position-2, APB height = 0 mm, Shroud Immersion = 0 mm)

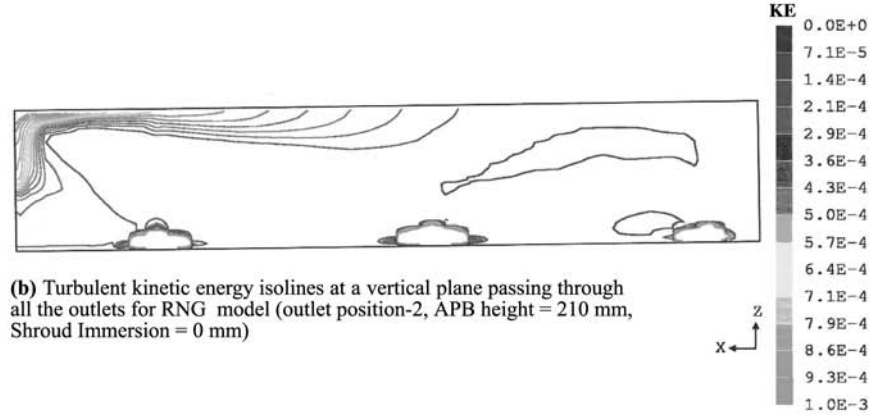

(b) Turbulent kinetic energy isolines at a vertical plane passing through all the outlets for RNG model (outlet position-2, APB height = 210 mm, Shroud Immersion = 0 mm)

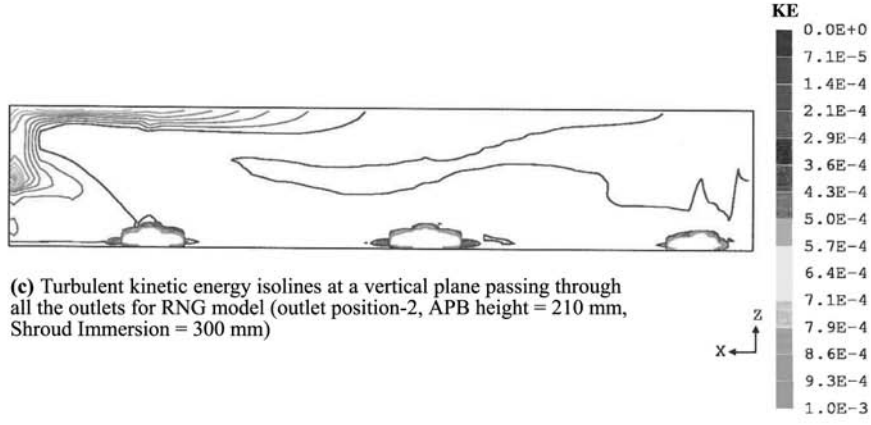

(c) Turbulent kinetic energy isolines at a vertical plane passing through all the outlets for RNG model (outlet position-2, APB height = 210 mm, Shroud Immersion = 300 mm)

Figure 8.

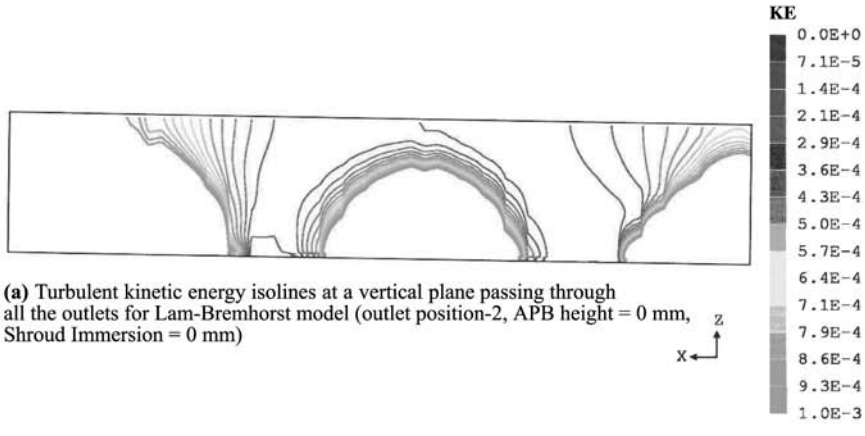

(a) Turbulent kinetic energy isolines at a vertical plane passing through all the outlets for Lam-Bremhorst model (outlet position-2, APB height = 0 mm, Shroud Immersion = 0 mm)

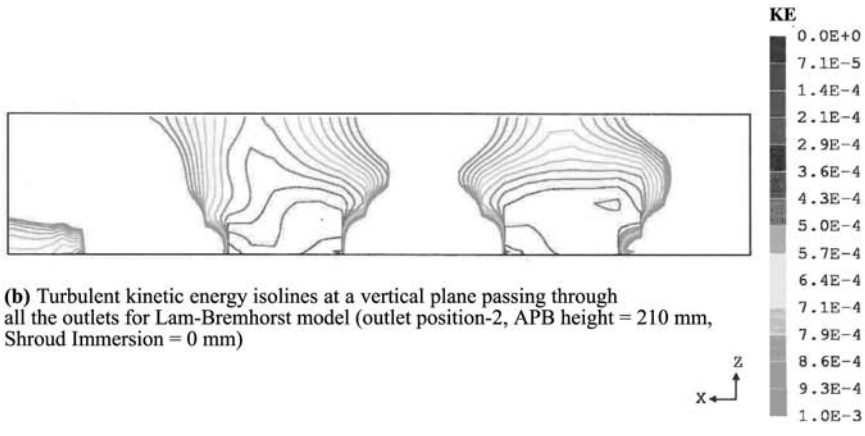

(b) Turbulent kinetic energy isolines at a vertical plane passing through all the outlets for Lam-Bremhorst model (outlet position-2, APB height = 210 mm, Shroud Immersion = 0 mm)

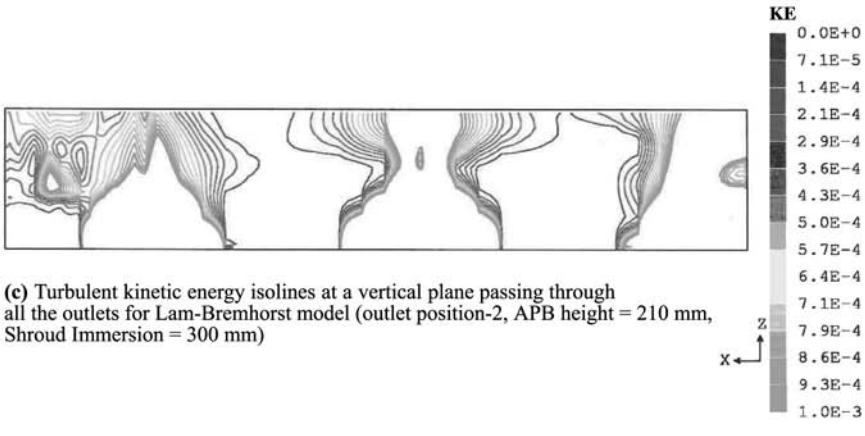

(c) Turbulent kinetic energy isolines at a vertical plane passing through all the outlets for Lam-Bremhorst model (outlet position-2, APB height = 210 mm, Shroud Immersion = 300 mm)

Figure 9.

in the tundish. Three of the six turbulence models (k-ε, Lam-Bremhorst and CEV) used for the simulation predict 300 mm to be the optimum shroud immersion depth.

It is evident from the present work that there exists physically optimum value for location of the outlets, height of the APB and shroud immersion depth for maximum values of the mean residence time and V_m/V_d. However, in order to decide the optimum values in geometrical parameters for a tundish one has to rely on experiments because the tundish fitted with an APB and a shroud is a fairly complex shaped geometrical device where the certainty of application of a particular turbulence model is questionable.

Note

1. *PHOENICS Users' Manual*, Version 3.2, CHAM Limited, UK.

References

Debroy, T. and Sychterz, J.A. (1985), "Numerical calculation of fluid flow in a continuous casting tundish", *Metallurgical Transactions*, Vol. 16B, pp. 497-504.

Ferziger, J.H. and Peric, M. (1999), *Computational Methods for Fluid Dynamics*, Springer, Berlin, pp. 279-86.

He, Y. and Sahai, Y. (1987), "The effect of tundish wall inclination on the fluid flow and mixing", *Metallurgical Transactions*, Vol. 18B, pp. 81-91.

Illegbusi, O.J. and Szekely, J. (1988), "Fluid flow and tracer dispersion in shallow tundishes", *Steel Research*, Vol. 59, pp. 399-405.

Illegbusi, O.J. and Szekely, J. (1989), "Effect of externally imposed magnetic field on tundish performance", *Ironmaking and Steelmaking*, Vol. 16, pp. 110-5.

Jha, P.K. and Dash, S.K. (2002), "Effect of outlet positions and various turbulence models on mixing in a single and multi-strand tundish", *Int. J. Num. Meth. Heat & Fluid Flow*, Vol. 12, pp. 560-84.

Jha, P.K., Dash, S.K. and Kumar, S. (2001), "Fluid flow and mixing in a six-strand billet caster tundish: a parametric study", *ISIJ International*, Vol. 41, pp. 1437-46.

Lam, C.K.G. and Bremhorst, K. (1981), "A modified form of the k-ε model for predicting wall turbulence", *Trans ASME Journal of Fluids Engineering*, Vol. 103, pp. 456-60.

Launder, B.E. and Spalding, D.B. (1972), *Mathematical Models of Turbulence*, Academic Press, London.

Levenspiel, O. (1972), *Chemical Reaction Engineering*, Wiley, New York, NY, pp. 253-64.

Madias, J., Martin, D., Ferreyra, M., Villoria, R. and Garamendy, A. (1999), "Design and plant experience using an advanced pouring box to receive and distribute the steel in a six strand tundish", *ISIJ Int.*, Vol. 39, pp. 787-94.

Mazumdar, D. and Guthrie, R.I.L. (1999), "The physical and mathematical modeling of continuous casting tundish systems", *ISIJ Int.*, Vol. 39, pp. 524-47.

Monson, D.J., Seegmiller, H.L., McConnaughey and Chen, Y.S. (1990), "Comparison of experiment with calculations using curvature – corrected zero and two equations turbulence models for a two-dimensional U-duct", *AIAA*, pp. 90-1484.

Morales, R.D., Diaz-Cruz, M., Palafox-Ramos, J., Lopez-Ramirez, S., Barreto-Sandoval, J. and de, J. (2000a), "Modeling steel flow in a three strand billet tundish using a turbulence inhibitor", *Steel Research*, Vol. 8, pp. 11-16.

Morales, R.D., Lopez-Ramirz, S., Palafox Ramos, J., Barreto-Sandoval, J., de, J. and Zacharias, D. (2000b), "Melt flow control in a multiple strand tundish using a turbulence inhibitor", *Metallurgical and Materials Trans.*, Vol. 31B, pp. 1505-15.

Singh, S. and Koria, S.C. (1993), "Model study of the dynamics of flow of steel melt in tundish", *ISIJ Int.*, Vol. 33, pp. 1228-37.

Singh, S. and Koria, S.C. (1995), "Study of fluid flow in tundishes due to different types of inlet streams", *Steel Research*, Vol. 66, pp. 294-300.

Szekely, J. and Themelis, N.J. (1971), *Rate Phenomena in Process Metallurgy*, Wiley, New York, NY, pp. 515-56.

Szekely, J., Illegbusi, O.J. and El-Kaddah, N. (1987), "The mathematical modeling of complex fluid flow phenomena in tundishes", *PhysicoChemical Hydrodynamics*, Vol. 9, pp. 453-72.

Tacke, K.H. and Ludwig, J.C. (1987), "Steel flow and inclusion separation in continuous casting tundishes", *Steel Research*, Vol. 58, pp. 262-70.

Xintian, L., Yaohe, Z., Baolu, S. and Weiming, J. (1992), "Flow behavior and filtration of steel melt in continuous casting tundish", *Ironmaking and Steelmaking*, Vol. 19, pp. 221-5.

Yahkot, Y. and Orszag, S.A. (1992), "Development of turbulence models for shear flows by a double expansion technique", *Phys. Fluids A*, Vol. 4, pp. 1510-20.

Yeh, J-L., Hwang, W-S. and Chou, C-L. (1992), "Physical modeling validation of computational fluid dynamics code for tundish design", *Ironmaking and Steelmaking*, Vol. 19, pp. 501-4.